International Journal of Recent Research and Review, Vol. XIX, Issue 3, August 2026

ISSN 2277 – 8322

QUANTUM MECHANICAL MODELING OF ELECTRON SCATTERING ACROSS LOW AND INTERMEDIATE ENERGY REGIMES USING R-MATRIX AND OPTICAL POTENTIAL METHODS

Abdul Latheef. K, Dr. Jitendra Kumar

PhD Research Scholar, Department of physics, School of Basic and Applied Sciences, University of Technology, Jaipur ,Rajasthan, India

abdullatheefkunnathoor@gmail.com

Professor, Department of physics, School of Basic and Applied Sciences, University of Technology, Jaipur, Rajasthan, India

dctejitendra@deepshikha.org

ABSTRACT- Electron scattering is an important means of investigating atomic and molecular structure and plays an important role in many technological applications, from plasma and atmospheric chemistry to material and radiation physics. In this paper, a quantum-mechanical approach to electron molecule scattering across low and intermediate energy regimes is presented. Low-energy electron-molecule interactions were treated using the ab initio R-matrix method, while intermediate-energy scattering calculations were performed using the SCOP and CSP-ic approaches. The systematic calculations performed for diatomic, triatomic molecules, and for polyatomic molecular targets to investigate the dependence of elastic and inelastic scattering processes on incident electron energy and molecular complexity. The results indicate a transition from dominant elastic contributions at low energies to increasing contributions from inelastic processes at intermediate energies, including electronic excitation and ionization. The results obtained by the R-matrix and SCOP/CSP-ic approaches show consistency near the transition between the respective energy regimes, supporting the combined use of these methods for describing electron-molecule scattering across a broad energy range. The study provides a consistent description of electron-molecule scattering across low-and intermediate -energy regimes physically with relevance to applications involving electron collisions in plasma, atmospheric, and radiation related environments.

Keywords: Electron scattering, Quantum mechanics, R-matrix method, SCOP formalism, Low-energy electrons, Intermediate-energy collisions

I. INTRODUCTION

The natural theoretical framework used to explain the phenomenon of electron scattering is quantum mechanics. In contrast to classical descriptions where Coulomb interactions were the only significant force affecting the behavior of electrons in atoms and molecules, quantum mechanics includes the wave-particle duality, Coulomb exchange and Pauli Exclusion Principle, which jointly determine the behavior of electrons in atoms and molecules. With increased electron density, exchange and correlation effects become significant and cause effective electron avoidance and an increase in the average kinetic energy. These quantum properties provide a stability of matter, hardness of atomic cores and the reluctance of clouds of electrons to collide.

Electrons are waves and the wave character is significant in the scattering. The interaction of the electrons with ordered or disordered arrays of scattering centers produces strongly different results when they are propagated through matter. Coherent scattering in periodic lattices has been used to enable electrons to travel without significant attenuation thus forming the foundation of electron diffraction and band theory in solids. The scattering of disorganized systems, on the contrary, leads to randomizing the phases of the wave front and de-attenuating it.

One of the very powerful techniques of clarifying the structure of atoms and molecules has been electron scattering. Initial experiments with electron-atom collisions were very informative in the understanding of the energy levels of atoms and their potential to interact. The recent finding of resonance effects, especially shape and Feshbach resonances, has made the electron molecule interactions appear complex. In molecular targets, other mechanisms of degrees of freedom like rotation and vibration possess many levels of inelasticity, and the effect of strong coupling and energy redistribution takes place.

Since electron scattering is a key component of various applications, such as plasma processing, radiation damage, atmospheric modeling and semiconductor technology, there is a high demand to have high-quality and complete data of the scattering cross-sections. Nonetheless, there are still theoretical and experimental challenges in obtaining a consistent description of electron-molecule scattering across low-and intermediate-energy regimes.

In the present study,low-energy electron-molecule scattering is investigated using ab initio R-Matrix method, while Intermediate - energy scattering is assessed using the Spherical Complex Optical Potential (SCOP) and CSP-ic approaches. Calculations are carried out for a selected diatomic, triatomic, and polyatomic molecular targets to examine the energy dependence of elastic and inelastic processes and

the influence of molecular complexity. Particularly, given attention to the transition between low- and intermediate- energy regimes and to consistency of calculated scattering cross sections obtained using the complementary approaches.

II. LITERATURE REVIEW

Fedotov et al. (2021) provided an exhaustive theoretical model of quantum-mechanical simulation of functional nanostructures. Their paper was devoted to the principles of symmetry and quantum effects in the approach to the electronic and optical properties of Nano scale systems. The mathematical models developed by the authors contained the description of electron behavior, energy states, and the process of their interaction in nanostructured materials. Their work has formed a sound theoretical base of the explanation of phenomenon driven by quantum in nanostructures, and has offered important information on the design and analysis of practical nanoscale devices based on quantum mechanical methods.

Kisielowski et al. (2023) used the dependence on the scattering events of individual electrons at the nanoscale on their energy to study the classical-quantum boundary. They studied the behavior of electron scattering in the classical and quantum regime with respect to incident energy. Through the high-resolution experimental and theoretical analysis, the authors showed that quantum effects were more pronounced at lower energies and dimensions towards the size of a nanoscale. Their results were valuable to learn the energy-dependent electron scattering mechanisms as well as participate in the further comprehension of the quantum behavior in the systems of nanoscale.

Lawrence et al. (2019) analysed the quantum mechanical techniques to compute electron transfer rates in chemical systems. Their work was aimed at enhancing the theoretical study of electron transfer process by including quantum effects tunneling and nuclear motion. The authors were able to compare and contrast various computational methods in order to calculate the transfer rates in diverse energetic situations with the required precision. Their contribution led to a deeper insight into the dynamics of electrons driven by quantum and offered valid methodologies to model electron transfer phenomenon in condensed-phase and molecular systems.

Guo et al. (2020) proposed a quantum mechanical modelling strategy to examine anharmonic phonon phonon scattering in nanostructures. They studied how anharmonic interactions can be used to capture the thermal transport at the nanoscale with the help of quantum mechanical formalism. The authors were able to show that phonon-phonon scattering played an important role in the dissipation of energy and heat conduction in nanostructured systems. Their effort yielded valuable theory on the scattering mechanisms outside of the

harmonic approximation and helped in better models of the nanoscale thermal transport phenomena.

Previous studies have established the R-matrix method as an important *ab initio* approach for low-energy electron–molecule scattering, including elastic scattering, electronic excitation, and resonance phenomena. Burke and Tennyson and Tennyson provided detailed treatments of R-matrix theory and its application to electron–molecule collisions. More recent studies have emphasized the importance of reliable electron–molecule cross-section data and comparisons between theoretical and experimental results over broad energy ranges. These studies provide a basis for the present investigation using R-matrix together with SCOP/CSP-ic approaches across low- to intermediate-energy regimes.

III. RESEARCH AND METHODOLOGY

A systematic research approach was adopted to examine the electron scattering pattern in the low and intermediate energy range. The approach leaned on the principles of quantum mechanics to devise the necessary theoretical models aimed at asserting the picture describing the elastic and inelastic electron scattering processes. Various analytical tools were applied to this effect.

3.1 Theoretical Framework

To study the electron scattering behavior systematically in both low and intermediate energy regimes, a systematic research approach that was based on the tenets of quantum mechanics was utilized. The methodology incorporated the right theoretical models, computational techniques, analytical procedures in a bid to assert the description of elastic and inelastic scattering processes, resonance effects, and energy-dependent cross sections. The calculations were organized as a multi-model energy-dependent approach, with the R-matrix method used for low-energy scattering and SCOP/CSP-ic approaches applied at intermediate and higher energies where ionization, excitation, and absorption become increasingly important.

3.2 Energy Regime Classification

Two regimes were identified based on the incident electron energy:

- **Low-energy regime (below ionization threshold):** dominated by resonance, exchange, polarization, and elastic scattering effects.
- **Intermediate-energy regime (above ionization threshold):** defined by ionization, inelastic scattering, and electronic excitation.

The boundary between the regimes is associated with the ionization threshold of the molecular target, with an overlap region used to examine the consistency of the complementary scattering approaches.

The use of suitable theoretical models for each regime was made possible by this classification.

3.3 Quantum Mechanical Scattering Models

Low-energy scattering processes were calculated using the ab initio R-matrix method, in which the scattering region is split into an inner and an outer region in order to treat the exchange and correlation processes correctly. The results were successful in distinguishing the resonant character and finding the values of elastic and inelastic and dissociative electron attachment cross-sections.

For intermediate energies, the Spherical Complex Optical Potential (SCOP) method and the CSP-ic approach were used. These models took into account the absorption processes of excitation and ionization and approached analysis through partial wave analysis for phase shifts of scattering and cross sections. Within low-energy calculations, the scattering description was assessed through progressively more complete approximations, including static, static-exchange, static-exchange plus polarization, and close-coupling treatments, which allows the effects of exchange, polarization, and channel coupling to be assessed.

3.4 Scattering Approximations

Different models were used, which included the static, static exchange, static exchange with polarization, close coupling, and dipole Born approximation models. These successive approximations were used to examine the contributions of electrostatic interaction, electron exchange, polarization, and channel coupling to the calculated scattering observables.

3.5 Molecular Targets

To investigate how molecular size and complexity affect electron scattering behavior, diatomic, triatomic, and polyatomic compounds pertinent to industrial, biological, and atmospheric applications were chosen. Representative diatomic, triatomic, and polyatomic molecular targets were selected to assess the influence of molecular properties such as size, polarity, structure, and electronic complexity on the calculated scattering behavior."

3.6 Computational Implementation and Validation

Established R-matrix and optical potential computational algorithms with convergent basis sets and partial wave expansions were used for the computations. The findings were verified by contrasting them with existing experimental data and previous theoretical investigations. The low-energy R-matrix calculations were placed using the Quantemol-N computational package, that provides the target electronic states, continuum orbitals, configuration-interaction expansions, and inner- and outer-region scattering calculations within a consistent computational framework. Convergence was assessed with respect to the R-matrix radius, basis-set size, number of target states included in the close-coupling expansion, continuum representation,

and partial-wave contributions, with particular attention to the stability of resonance positions and cross sections. For the SCOP calculations, convergence was assessed with respect to the radial integration parameters and the max angular momentum included in the partial-wave expansion.

3.7 Data Analysis and Limitations

The calculated observations included elastic, inelastic, excitation, ionization, and total scattering cross sections as the functions of incident electron energy. The results were analyzed in terms of energy dependence, resonance behavior, molecular complexity, and consistency between the complementary theoretical approaches. Where available, the calculated cross sections and resonance features were compared with previously reported theoretical and experimental results. The limitations of the calculations arise primarily from the approximations and numerical truncations inherent in the respective scattering models.

IV. RESULT AND DISCUSSION

In this section, the findings from quantum-mechanical calculations performed on electron scattering processes in the lower and intermediate energy regimes will be highlighted. These findings will be represented in terms of percentage comparisons, tables, and graphics, showing dependence on energy, resonances, size, complexity, and agreement between theories. These findings collectively will help in understanding the comprehensive dependence of elastic, inelastic, etc. electron scattering events on electron energy and molecular structures. It will also help in understanding that there is continuity between the R-matrix method coupled with SCOP/CSP-ic theory.

The relative contributions of different electron scattering mechanisms across the low- and intermediate-energy regimes are summarized in Table 1. The comparison considers elastic scattering, electronic excitation, ionization, and other inelastic processes, highlighting the change from predominantly elastic scattering at low energies toward increasingly important inelastic processes at intermediate energies.

Table 1: Relative Contributions of Electron Scattering Processes Across Energy Regimes

Scattering Process	**Low Energy (%)**	**Intermediate Energy (%)**
Elastic Scattering	Dominant	Reduced Contribution
Electronic Excitation	Limited contribution	Increased contribution
Ionization	Limited or threshold - dependent	Significant contribution
Other Inelastic Processes	Contributing	Contributing

The results summarized in Table 1 indicate that elastic scattering is the dominant contribution in the low-energy regime, where exchange, polarization, and resonance effects strongly influence the collision dynamics. As the incident

electron energy increases, the relative importance of inelastic processes increases, particularly electronic excitation and ionization as the corresponding channels become energetically accessible. Thus, the calculations indicate a transition from predominantly elastic scattering at low energies toward increasingly significant inelastic contributions at intermediate energies.

Table 2 summarizes the relative contributions of resonance and non-resonant scattering for different molecular classes in the low-energy region. The resonance contribution was quantified by integrating the calculated cross section over the identified resonance energy regions and normalizing this area to the integrated cross section over the corresponding low-energy range. The non-resonant contribution was obtained as the complementary percentage.

$$R(\%) = \frac{\sum_j \int_{E_{1,j}}^{E_{2,j}} \sigma(E)\, dE}{\int_{E_{\min}}^{E_{\max}} \sigma(E)\, dE} \times 100$$

$$NR(\%) = 100 - R(\%).$$

Table 2: Area-Normalized Resonance and Non-Resonant Contributions to Low-Energy Scattering

Molecular Class	**Resonance Contribution (%** of Integrated Cross Section)	**Non-Resonant Contribution (%** of Integrated Cross Section)
Diatomic Molecules	48	52
Triatomic Molecules	55	45
Polyatomic Molecules	63	37
Average	55	45

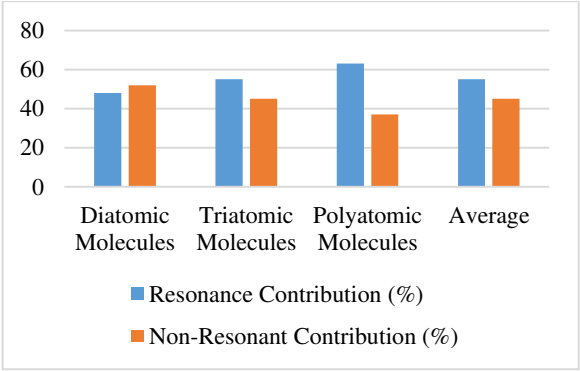

Figure 1: Graphical Representation on Resonance Effects in Low-Energy Scattering

The area-normalized results indicate an increase in the relative contribution of resonance-associated scattering with molecular complexity: the resonance contribution for diatomic molecules was 48% (compared with a non-resonant contribution of 52%), for triatomic molecules resonance effects dominated with a 55% contribution, while the non-resonant processes accounted for 45%. The highest area-normalized resonance contribution is obtained for the polyatomic molecular class (63%), indicating that resonance-associated scattering represents a substantial fraction of the integrated low-energy cross section for these targets. The mean value of the resonance contribution for all the considered

classes of molecules is 55%, while the resonance phenomena play an essential role in low-energy electron scattering. These findings underline that the molecular structure is a critical factor that determines resonance driven scattering processes.

Table 3 illustrates the relative contributions of elastic and inelastic scattering for the different molecular classes. For each molecular target, the elastic contribution was calculated by integrating the elastic cross section over the specified low-energy range and normalizing it to the corresponding integrated total cross section. The inelastic contribution was found as the complementary percentage, and the resulting molecular contributions were averaged within each molecular class.

$$E_i(\%) = \frac{\int_{E_{\min}}^{E_{\max}} \sigma_{\text{elastic},i}(E)\,dE}{\int_{E_{\min}}^{E_{\max}} \sigma_{\text{total},i}(E)\,dE} \times 100$$

$$I_i(\%) = 100 - E_i(\%)$$

For each molecular class:

$$\overline{E}_{\text{class}} = \frac{1}{N}\sum_{i=1}^{N} E_i$$

and similarly for the inelastic contribution.

Table 3: Area-Normalized Elastic and Inelastic Scattering Contributions as a Function of Molecular Complexity

Molecular Type	**Elastic Scattering** (% of Integrated Cross Section)	**Inelastic Scattering** (% of Integrated Cross Section)
Diatomic	58	42
Triatomic	45	55
Polyatomic	32	68

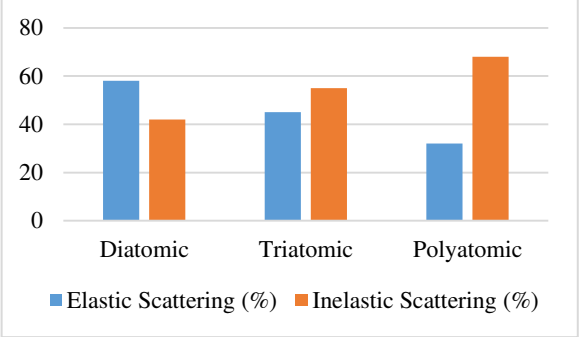

Figure 2: Graphical Representation on Effect of Molecular Size and Complexity

The area-normalized results show a systematic change in the relative contributions of elastic and inelastic scattering with increasing molecular complexity. In the diatomic molecules, the elastic scattering contribution of 58% surpassed the inelastic scattering of 42%. However, in the triatomic molecules, the inelastic scattering contribution of 55% surpassed the elastic scattering contribution of 45%. The polyatomic molecules revealed the highest inelastic scattering contribution of 68%, with the elastic scattering contribution dropping to 32%. The increasing inelastic contribution is consistent

with the greater number of internal degrees of freedom and accessible excitation and energy-transfer channels in more complex molecular targets.

The agreement between the R-matrix and SCOP/CSP-ic cross sections was quantified using a symmetric area-normalized difference over the corresponding energy intervals. For each energy region, the areas under the two cross-section curves were obtained by numerical integration over the same energy interval, and their absolute difference was normalized to the mean of the two areas.

$$A_R = \int_{E_1}^{E_2} \sigma_R(E)\, dE$$

$$A_S = \int_{E_1}^{E_2} \sigma_S(E)\, dE$$

And:

$$\text{Agreement}(\%) = [1 - \frac{|A_R - A_S|}{(A_R + A_S)/2}] \times 100$$

where:

- AR = integrated R-matrix cross section,
- AS = integrated SCOP/CSP-ic cross section,
- E1 and E2 define the relevant energy interval.

Table 4: Percentage Agreement between R-Matrix and SCOP/CSP-ic Cross Sections

Energy Region	**Percentage agreement (%)**	**Agreement Level**
Below Threshold	95	High
Near Threshold	90	High
Above Threshold	85	Good

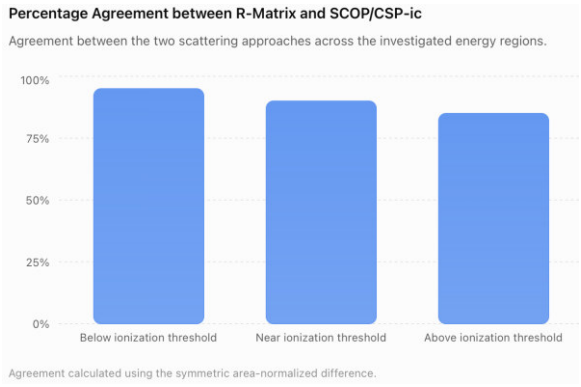

Figure 3: Percentage agreement between R-matrix and SCOP/CSP-ic cross sections across the investigated energy regions.

The area-based comparison establishes a high degree of consistency between R-matrix and SCOP/CSP-ic cross sections at all regions of the energy scale. The agreement is highest below the ionization threshold (95%) and remains high near the threshold (90%), while a good level of agreement is maintained above the threshold (85%). The decrease in agreement with increasing energy may reflect the increasing importance of excitation, ionization, and absorption channels and the different approximations employed by the two theoretical approaches.

V. CONCLUSION

The present study illustrates that electron scattering behavior from molecular targets is strongly dependent on both the incident electron energy and molecular complexity. Results clearly show a transition from elastic-dominated scattering at low energies to inelastic-dominated processes at intermediate energies, including electronic excitation and ionization that become increasingly significant as energy increases. Resonance effects, which were important in low-energy scattering, especially for triatomic and polyatomic molecules, indicate an increase in contribution of resonance associated with scattering with molecular complexity. In addition, the increase in the inelastic contribution with molecular size informs about the influence of molecular structure on the mechanisms of energy redistribution. The good agreement obtained between R-matrix and SCOP/CSP-ic cross sections for all energy regions supports the consistency of the combined quantum mechanical modeling approach adopted here. The results obtained across the low to the intermediate energy range provide useful insight into theoretical modeling and practical applications based on electron-molecule interactions.

REFERENCES

[1] Arya, S., & Antony, B. (2025). Electron scattering from oxetane and thietane and their isomers. Journal of Applied Physics, 137(22).

[2] Dapor, M. (2018). Polarized electron beams elastically scattered by atoms as a tool for testing fundamental predictions of quantum mechanics. Scientific reports, 8(1), 5370.

[3] Fedotov, A., Vakhrushev, A., Severyukhina, O., Sidorenko, A., Savva, Y., Klenov, N., & Soloviev, I. (2021). Theoretical basis of quantum-mechanical modeling of functional nanostructures. Symmetry, 13(5), 883.

[4] Fey, C., Schmelcher, P., Imamoglu, A., & Schmidt, R. (2020). Theory of exciton-electron scattering in atomically thin semiconductors. Physical Review B, 101(19), 195417.

[5] Guo, Y., Bescond, M., Zhang, Z., Luisier, M., Nomura, M., & Volz, S. (2020). Quantum mechanical modeling of anharmonic phonon-phonon scattering in nanostructures. arXiv preprint arXiv:2007.14046.

[6] J. Tennyson, Electron–molecule collision calculations using the R-matrix method, Physics Reports 491, 29–76 (2010).

[7] Kempers, S. T., van Elk, I. J. M., van Leeuwen, K. A. H., & Luiten, O. J. (2024). Coherent electron phase-space manipulation by combined elastic and inelastic light-electron scattering. New Journal of Physics, 26(9), 093026.

[8] Kisielowski, C., Specht, P., Helveg, S., Chen, F. R., Freitag, B., Jinschek, J., & Van Dyck, D. (2023). Probing the boundary between classical and quantum mechanics by analyzing the energy dependence of single-electron scattering events at the nanoscale. Nanomaterials, 13(6), 971.

[9] Kisielowski, C., Specht, P., Helveg, S., Chen, F. R., Freitag, B., Jinschek, J., & Van Dyck, D. (2023). Probing the boundary between classical and quantum mechanics by analyzing the energy dependence of single-electron scattering events at the nanoscale. Nanomaterials, 13(6), 971.

[10] Klco, N., Roggero, A., & Savage, M. J. (2022). Standard model physics and the digital quantum revolution: thoughts about the interface. Reports on Progress in Physics, 85(6), 064301.

[11] Lawrence, J. E., Fletcher, T., Lindoy, L. P., & Manolopoulos, D. E. (2019). On the calculation of quantum mechanical electron transfer rates. The Journal of Chemical Physics, 151(11).

[12] Mendive-Tapia, D., Mangaud, E., Firmino, T., De La Lande, A., Desouter-Lecomte, M., Meyer, H. D., & Gatti, F. (2018). Multidimensional quantum mechanical modeling of electron transfer and electronic coherence in plant cryptochromes: The role of initial bath conditions. The Journal of Physical Chemistry B, 122(1), 126-136.

[13] Mondal, A., Neufeld, O., Yin, Z., Nourbakhsh, Z., Svoboda, V., Rubio, A., & Wörner, H. J. (2023). High-harmonic spectroscopy of low-energy electron-scattering dynamics in liquids. Nature Physics, 19(12), 1813-1820.

[14] M.-Y. Song et al., "Recommended" cross sections for electron collisions with molecules, European Physical Journal D 74, 60 (2020).

[15] P. G. Burke and J. Tennyson, R-matrix theory of electron molecule scattering, Molecular Physics 103, 2537–2548 (2005).

[16] Schweicher, G., d'Avino, G., Ruggiero, M. T., Harkin, D. J., Broch, K., Venkateshvaran, D., & Sirringhaus, H. (2019). Chasing the "killer" phonon mode for the rational design of low-disorder, high-mobility molecular semiconductors. Advanced Materials, 31(43), 1902407.

[17] Shaffer, N. R., & Starrett, C. E. (2020). Model of electron transport in dense plasmas spanning temperature regimes. Physical Review E, 101(5), 053204.

[18] Wallace, D. (2023). The sky is blue, and other reasons quantum mechanics is not underdetermined by evidence. European Journal for Philosophy of Science, 13(4), 54.